

Influence of local carbon fibre orientation on the water transport in the gas diffusion layer of polymer electrolyte membrane fuel cells

Authors

Henning Markötter^{a,b,*}, Katja Dittmann^b, Jan Haußmann^c, Robert Alink^d, Dietmar Gerteisen^d, Heinrich Riesemeier^e, Joachim Scholta^c, John Banhart^{a,b}, Ingo Manke^b

Author affiliations

- a) Technische Universität Berlin (TUB), Straße des 17. Juni 135, 10623 Berlin, Germany
- b) Helmholtz-Zentrum Berlin (HZB), Hahn-Meitner-Platz 1, 14109 Berlin, Germany
- c) Zentrum für Sonnenenergie- und Wasserstoff-Forschung Baden Württemberg (ZSW), Helmholtzstraße 8, 89081 Ulm, Germany
- d) Fraunhofer Institut für Solare Energiesysteme (ISE), Heidenhofstr. 2, 79110 Freiburg, Germany
- e) Bundesanstalt für Materialforschung und -prüfung (BAM), Unter den Eichen 87, 12205 Berlin, Germany

*corresponding author

present/permanent address:

Helmholtz-Zentrum Berlin, Hahn-Meitner-Platz 1, 14109 Berlin, Germany

phone: +49 30 8062 42826

henning.markoetter@helmholtz-berlin.de

Keywords (max. 6 keywords)

Polymer electrolyte membrane fuel cell, gas diffusion layer, perforation, liquid water transport, local fibre structure, radiography combined with tomography

Abstract

We used synchrotron X-ray imaging to investigate the influence of local fibre structures of gas diffusion layers (GDL) in polymer electrolyte membrane fuel cells on the transport of water. Two different measurement techniques, namely in-situ radiography and ex-situ tomography, were combined to reveal the structure-

properties relationships between the three-dimensional fibre arrangement and the water flow. We found that the orientation of the local carbon fibres strongly affects the direction of liquid water transport. The carbon fibres act as guiding rails for the water droplets. These findings provide completely new ideas how gas diffusion media in various types of fuel cells could be designed, in order to optimise transport pathways for liquid water and therefore increase cell performance.

1 Introduction

Polymer electrolyte membrane fuel cells (PEMFCs) are currently the most promising fuel cell type for automotive applications. Air can be used on the cathode side, implying that only hydrogen gas has to be carried on board of a vehicle. PEMFCs also exhibit a dynamic performance in a wide range of operation parameters [1, 2]. However, water management is still one of the problems that prevent a broad establishment of PEMFCs in the automotive sector. A dry membrane loses proton conductivity whereas upon flooding with water the gas diffusion layer (GDL) gets blocked and the gas supply ceases [3], which results in an inhomogeneous current density affecting also the materials lifetime. Therefore, an effective removal of liquid water from the gas diffusion layer is a prerequisite for optimal performance as well as for stable fuel cell operation [4-11].

This article addresses the question how water transport is conducted in the local carbon fibre structure of a SGL Sigracet[®] 25BC, which is common in this fuel cell type [12]. The in-situ water transport in perforated gas diffusion layers was investigated during operation by synchrotron X-ray radiography that provides a high enough temporal and spatial resolution to examine even the small structural details of the gas diffusion layers in real time [13-15].

2 Experiments

2.1 In-situ radiography

The in-situ experiments were carried out using a PEMFC with an active area of $100 \times 100 \text{ mm}^2$ equipped with a three-fold serpentine flow field with a channel width of 0.8 mm separated by 0.9 mm wide ribs. The cathodic GDL (SGL 25 BC) was laser-perforated with a diameter of about $210 \mu\text{m}$ separated by a distance of 1 mm [16, 17]. Perforation was conducted with a focused Nd:YAG laser beam performing

circular movements. The perforations in the GDL were also located in the rib regions of the flow field. The distance between the edges of the channel and the perforations was about 200 μm (see Figure 2, image A).

A cut out with a diameter of 10 mm was drilled into the end plates of the fuel cell to ensure high transmission of the X-rays within the field of view. This raises the sensitivity to water located in the cell components, such like GDL and the gas channel system. The cell was kept at a temperature of 55°C and was supplied on both sides with preheated hydrogen and air having a relative humidity of 75% (@55°C). The radiographic images presented in Figure 1a, Figure 2 and Figure 3a were taken while operating the cell at 0.5 A/cm² current density. The hydrogen and air flow rates were set to 1 and 4 standard litres per minute.

The measurements were performed at the imaging beamline “BAMline” of the synchrotron electron storage ring “Bessy II” in Berlin, Germany. The observed field of view was 8.8 × 5.9 mm with a pixel size of 2.2 μm according to the detector resolution of 4008 × 2672 pixel. Images were acquired every 7s. The photon energy of 15 keV was selected with a W/Si double multilayer monochromator with an energy resolution $\Delta E/E$ of 1.5%.

The beam transmission was calculated via an image of the plain beam without the cell (flat field). The cell was radiographed during operation to capture the transport dynamics of the evolving liquid product water in the cell components. The amounts of water were quantified by combination with a radiographic image of the dry cell before operation.

2.2 Ex-situ tomography

After the dynamic radiographic experiments the cell was disassembled and the visualized area of the MEA including the anodic and cathodic MPL/GDL cut out in a circular shape of 7 mm diameter. The sample size selected allows for tomographic measurements with a voxel size of 2.2 μm . The extracted material was tomographed to study the GDL structure in all three dimensions. This technique allows a tomographic material analysis even of application-oriented fuel cells of this (large) size. A tomography with this resolution of the complete cell is only possible using a specially adapted smaller fuel cell [14, 18, 19].

The radiographic and tomographic image data has been matched in order to compare radiographically acquired water transport dynamics with the tomographically

captured three-dimensional structure. An overview of a matched area is given in Figure 1 showing a cut out of the radiographic image (a) and the corresponding tomographic 3D reconstruction of the GDL material (b).

3 Results

During cell assembly the GDL was positioned, so that the perforations are located at the rib structure of the flow field. In earlier work it was found that cracks in the MPL are initial points of liquid water transport paths through the GDL [20]. In the present case, the perforations play a similar role as the cracks: They yield as accumulation points for liquid water as was previously shown by Alink et al. and Markötter et al. [16, 17]. The emerging product water then moves from the perforations through the GDL into the channel, from where droplets are removed regularly by the streaming gas. The water is always transported through the same passage. Figure 2 shows the water distribution at five moments and the related amount of water displayed vs. time. The image inset in the graph shows the area, at which the average water depth was measured, which includes the perforation, a small passage to the channel and the area of the maximum droplet dimensions.

As becomes visible in Figure 2, showing hole #2 (see Figure 3), a droplet first builds up and is then carried away after some time by the streaming gas. This takes place periodically roughly every 80 seconds, resulting in significant decrease of the measured water depth. The droplet grows at a rate of 73 ± 5 pl/s, as derived from the slopes of the graph in Figure 2. The average water depth is also subject to small variations due to water transport in the channel, but never exceeded $300 \mu\text{m}$ throughout the complete measurement.

The SGL 25BC material consists of a non-woven structure with a material thickness of $235 \mu\text{m}$. The perforated cathodic GDL including the MEA and anodic GDL was investigated tomographically. A row of four perforations is presented in Figure 3. During the radiographic investigations, a complete filling of the perforations during fuel cell operation was observed. All the perforations (#1-4) fill up with liquid water, which is subsequently transported in-plane towards the channel (see Figure 3a).

The morphology of the perforation can not only be seen in the tomography but is also reflected by the water agglomerations in the radiography. Blue arrows in Figure 3a and b highlight the imperfect hole shape in the radiographic as well as in the tomographic measurements, thus allowing for an allocation and assignment of the

water and the perforations. The water is transported from the filled holes in-plane through the GDL towards the channel, thereby feeding droplets at the channel wall, one for each hole in the GDL. The principle of water transport is sketched in a side view in Figure 3d.

The area between the holes and the droplets (see for example the green arrows in Figure 3) is now analysed in detail. It was found that for each individual hole the liquid water always takes the same transport path from the hole to the channel.

A comparison to the tomography shows that the carbon fibre orientation in the first layers (facing the channel / rib) of the GDL coincides with the liquid water transport paths. In Figure 3c, the first carbon fibres are overlaid onto the water distribution of the radiography in order to emphasise the correlation between fibre orientation and water flow direction. At hole #1 a larger adjacent pore space is first being filled (see encircled area in Figure 3b and c) and the liquid water pathway is not yet completely build up at the time presented (4:47 min:s). At the other holes a droplet is already built up in the channel. The fibres around hole #2 and #4 direct the water to the top left, #3 rather directly towards the channel.

4 Discussion

The water discharge is carried out through the pore network of the GDL, which is strongly correlated with the carbon fibre orientation, i.e. the possible water transport paths are defined by the orientation of the local carbon fibres. However, although other paths are still available, water seems to prefer the well-defined paths formed by the fibres. This effect might be enhanced by a non-homogeneous distribution of hydrophobic PTFE. Parts of the fibres remain without PTFE on the surface. This causes hydrophilic spots and the water droplets might move along these hydrophilic spots although other free space is available and provides possible paths to the channel.

Mostly the fibres in the first layers of the GDL dominate the transport direction of the liquid water that has accumulated in the perforations. This can be explained by the reduced temperature at the flow field ribs that serve as condensation points for the water. The contact angle of the graphite bipolar plate was determined to be 55° , which is lower than that of the carbon fibres. Thus most water is preferably located at the top layer of the GDL. This is supported by earlier studies on water distribution in

PEMFCs where strong water accumulations in the GDL were found directly at the rib structure [14].

5 Conclusions and Outlook

Our study demonstrates that the orientation of the fibres is strongly influencing the water flow direction. The carbon fibres in the upper layers of the GDL act as guiding pathways for the water droplets.

This can be used, for example, to counteract specific weak points in the flow field geometry and to optimise the overall performance of fuel cells in general. A GDL with an artificially defined orientation of fibres in the top layer might be able to transport product water accumulations into the channel more easily. Therefore, the fibres in the top layer of the GDL should be oriented perpendicular to the local channel orientation. Considering, as for the presented measurements, a meander flow field with mostly horizontally aligned channels, the fibres in the top layer should be oriented vertically in order to ensure an optimal liquid water removal, which provides more available pore volume for the gas supply and results in more stable operation conditions [3]. These findings are not only important for the optimisation and development of GDL materials, but also for modelling the water transport [21]. In future we will analyse the effect of hydrophobicity on the correlation between GDL fibre orientation and water transport.

Acknowledgement

The assistance of the beamline scientists of the BAMline Thomas Wolk and Ralf Britzke is gratefully acknowledged. Funding of the project PEM-CaD (grant number: 03SF0360B) by the Federal Ministry of Education and Research (BMBF) is gratefully acknowledged.

References

- [1] L. Carrette, K.A. Friedrich, U. Stimming, Fuel Cells - Fundamentals and Applications, Fuel Cells, 1 (2001) 5-39.
- [2] C.-Y. Wang, Two-phase flow and transport, in: W. Vielstich, A. Lamm, H.A. Gasteiger (Eds.) Handbook of Fuel Cells – Fundamentals, Technology and Applications, vol. 3, John Wiley & Sons, Chichester, 2003, pp. 337–347.
- [3] J.P. Owejan, T.A. Trabold, M.M. Mench, Oxygen transport resistance correlated to liquid water saturation in the gas diffusion layer of PEM fuel cells, International Journal of Heat and Mass Transfer, 71 (2014) 585-592.

- [4] V.P. Schulz, J. Becker, A. Wiegmann, P.P. Mukherjee, C.Y. Wang, Modeling of two-phase behavior in the gas diffusion medium of PEFCs via full morphology approach, *J Electrochem Soc*, 154 (2007) 419-426.
- [5] X. Zhu, P.C. Sui, N. Djilali, Dynamic behaviour of liquid water emerging from a GDL pore into a PEMFC gas flow channel, *J Power Sources*, 172 (2007) 287-295.
- [6] U. Pasaogullari, P.P. Mukherjee, C.Y. Wang, K.S. Chen, Anisotropic heat and water transport in a PEFC cathode gas diffusion layer, *J Electrochem Soc*, 154 (2007) 823-834.
- [7] I.E. Baranov, S.A. Grigor'ev, I. Nikolaev, V.N. Fateev, Mass transfer in porous systems, flooded in part with water, of gas diffusion and catalytic layers of the cathode of a fuel cell with a solid polymer electrolyte, *Russ. J. Electrochem.*, 42 (2006) 1325-1331.
- [8] J.H. Nam, M. Kaviany, Effective diffusivity and water-saturation distribution in single- and two-layer PEMFC diffusion medium, *International Journal of Heat and Mass Transfer*, 46 (2003) 4595-4611.
- [9] S. Litster, D. Sinton, N. Djilali, Ex situ visualization of liquid water transport in PEM fuel cell gas diffusion layers, *J Power Sources*, 154 (2006) 95-105.
- [10] M. Mortazau, K. Tajiri, Liquid water breakthrough pressure through gas diffusion layer of proton exchange membrane fuel cell, *International Journal of Hydrogen Energy*, 39 (2014) 9409-9419.
- [11] T. Sasabe, P. Deevanhxay, S. Tsushima, S. Hirai, Investigation on the effect of microstructure of proton exchange membrane fuel cell porous layers on liquid water behavior by soft X-ray radiography, *J Power Sources*, 196 (2011) 8197-8206.
- [12] H. Li, Y. Tang, Z. Wang, Z. Shi, S. Wu, D. Song, J. Zhang, K. Fatih, J. Zhang, H. Wang, Z. Liu, R. Abouatallah, A. Mazza, A review of water flooding issues in the proton exchange membrane fuel cell, *J Power Sources*, 178 (2008) 103-117.
- [13] A. Bazylak, Liquid water visualization in PEM fuel cells: A review, *International Journal of Hydrogen Energy*, 34 (2009) 3845-3857.
- [14] P. Krüger, H. Markötter, J. Haussmann, M. Klages, T. Arlt, J. Banhart, C. Hartnig, I. Manke, J. Scholta, Synchrotron X-ray tomography for investigations of water distribution in polymer electrolyte membrane fuel cells, *Journal of PowerSources*, 196 (2011) 5250-5255.
- [15] I. Manke, C. Hartnig, M. Grünerbel, W. Lehnert, N. Kardjilov, A. Haibel, A. Hilger, J. Banhart, H. Riesemeier, Investigation of water evolution and transport in fuel cells with high resolution synchrotron x-ray radiography, *Appl Phys Lett*, 90 (2007) 174105.
- [16] R. Alink, J. Haußmann, H. Markötter, M. Schwager, I. Manke, D. Gerteisen, The influence of porous transport layer modifications on the water management in polymer electrolyte membrane fuel cells, *J Power Sources*, 233 (2013) 358-368.
- [17] H. Markötter, R. Alink, J. Haußmann, K. Dittmann, T. Arlt, F. Wieder, C. Tötze, M. Klages, C. Reiter, H. Riesemeier, J. Scholta, D. Gerteisen, J. Banhart, I. Manke, Visualization of the water distribution in perforated gas diffusion layers by means of synchrotron X-ray radiography, *International Journal of Hydrogen Energy*, 37 (2012) 7757-7761.
- [18] H. Markötter, I. Manke, P. Krüger, T. Arlt, J. Haussmann, M. Klages, H. Riesemeier, C. Hartnig, J. Scholta, J. Banhart, Investigation of 3D water transport paths in gas diffusion layers by combined in-situ synchrotron X-ray radiography and tomography, *Electrochem Commun*, 13 (2011) 1001-1004.
- [19] J. Haußmann, H. Markötter, R. Alink, A. Bauder, K. Dittmann, I. Manke, J. Scholta, Synchrotron radiography and tomography of water transport in perforated gas diffusion media, *J Power Sources*, 239 (2013) 611-622.

[20] H. Markötter, J. Haußmann, R. Alink, C. Tötze, T. Arlt, M. Klages, H. Riesemeier, J. Scholta, D. Gerteisen, J. Banhart, I. Manke, Influence of cracks in the microporous layer on the water distribution in a PEM fuel cell investigated by synchrotron radiography, *Electrochem Commun*, 34 (2013) 22-24.

[21] K. Seidenberger, F. Wilhelm, J. Haußmann, H. Markötter, I. Manke, J. Scholta, Grand canonical Monte Carlo study on water agglomerations within a polymer electrolyte membrane fuel cell gas diffusion layer, *J Power Sources*, 239 (2013) 628-641.

Figure 1: Overview of the matched segment showing the perforated SGL 25 BC GDL; a) radiographic image with water distribution obtained during operation; b) tomographic 3D reconstruction of the GDL fibres.

Figure 2: Water evolution and discharge quantified by X-ray radiography right after starting operation ($t=0$).

Figure 3: a: Still radiograph of the water dynamics at 4:47 (min:s) after start of operation; b: View onto the reconstructed GDL structure; c: Radiography with sketched fibre orientations of the top layer; d: Sketch of the visualised area in a side view.

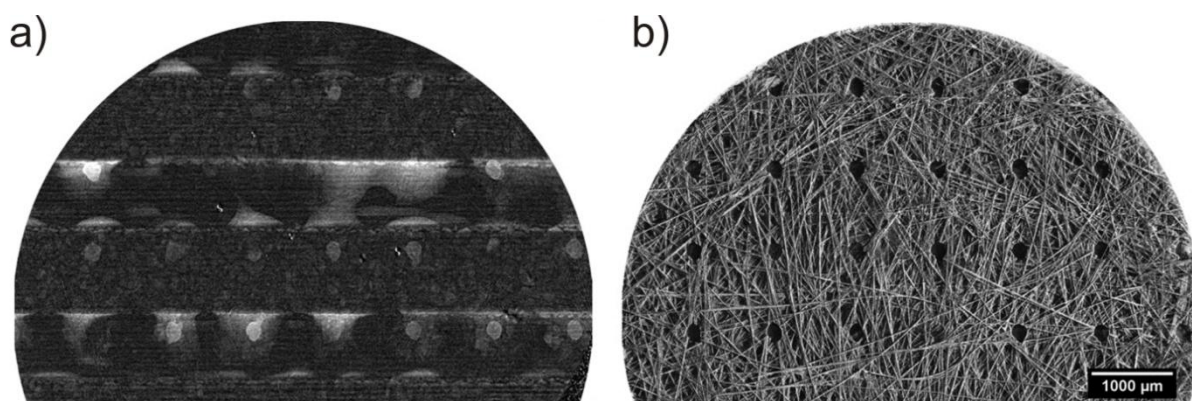


Figure 1

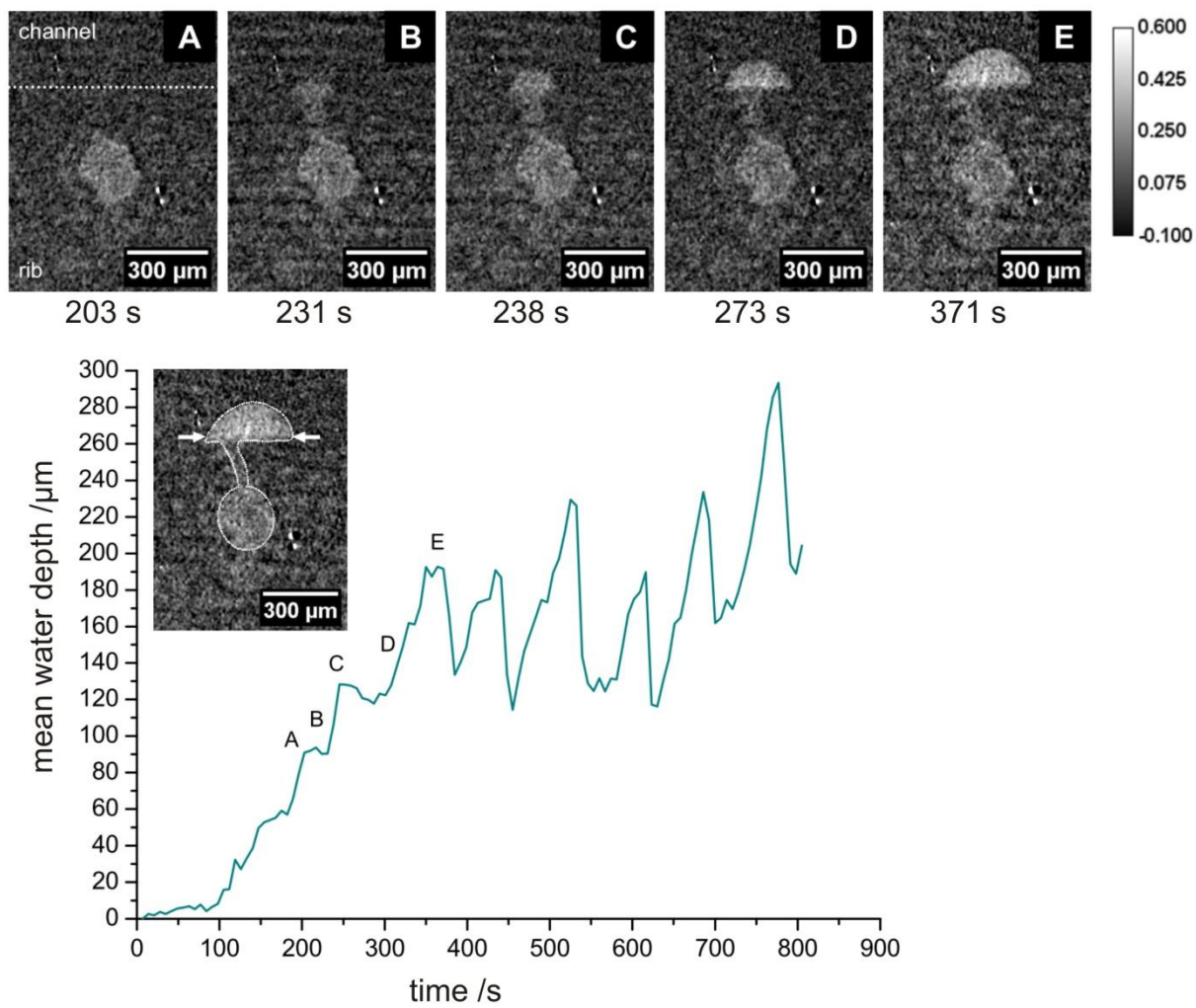


Figure 2

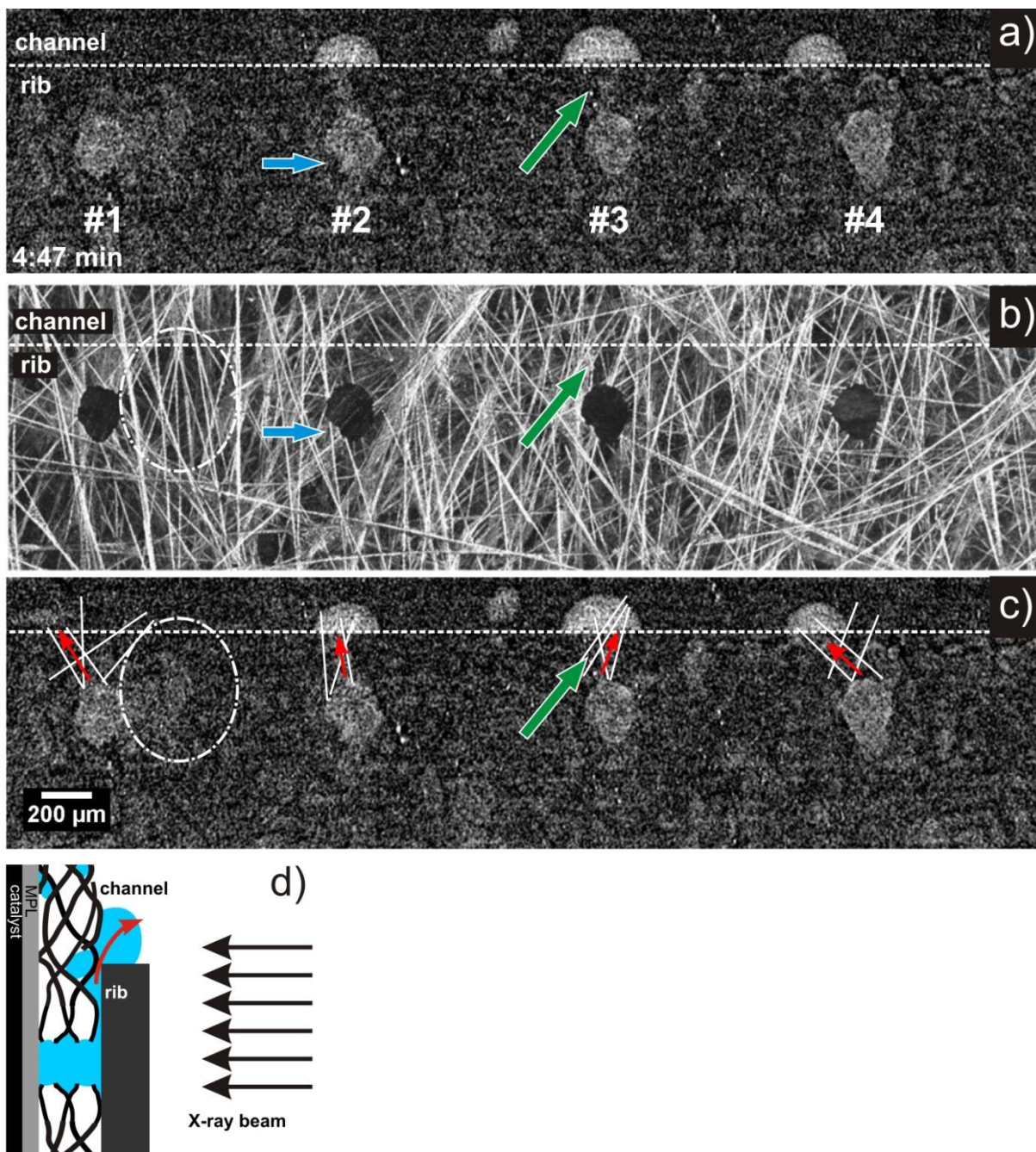
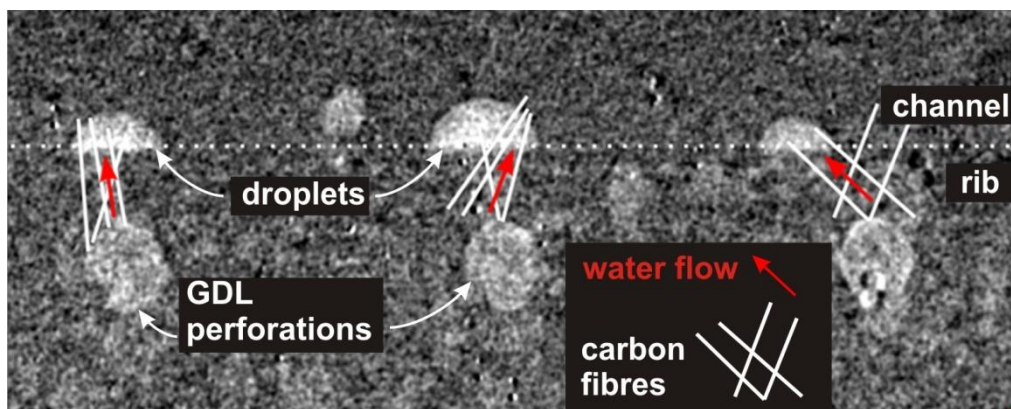


Figure 3



Graphical abstract

Highlights

- Ex-Situ tomography and In-Situ radiography of water transport in 3D fibre structure
- Local fibre orientation strongly affects liquid water transport direction
- Continuous liquid water transport quantified via droplet growth